modes is replaced by an integral.

[9]E. T. Jaynes and F. W. Cummings, Proc. IEEE 51, 89 (1963).

[10]When we describe spontaneous emission, we will allow the cavity to become very large. We will assume that in that limit n also becomes very large so that in that limit ϵ approaches a constant finite value representing a finite strength.

[11]An excellent review article on the Stark effect is A. M. Bonch-Bruevich and V. A. Khodovoi, Usp. Fiz. Nauk 93, 71 (1967)[Soviet Phys. Usp. 10, 637 (1968)].

[12]This technique was apparently first used for this type of problem by G. Kallen, in *Handbuch der Physik*, edited by S. Flügge (Springer, Berlin, 1958), Vol. V. It has been used several times since for simple spontaneous emission.

[13]Numerical calculations indicate that the field strength $\epsilon = A$ would require a laser beam tuned to resonance with an intensity of about 1 W/cm^2 for the sodium D lines.

[14]It is interesting to note that this integral is not divergent if we retain the retardation rather than making the dipole approximation, though it does not appear to give the correct answer for the Lamb shift. See C. R. Stroud, Jr., Ph.D. thesis, Washington University, St. Louis, Mo. (unpublished), for a detailed treatment for the 1s and 2p states in hydrogen. There it is shown that there is a small correction to exponential decay which goes at t^{-2} for sufficiently long times.

[15]We have used exactly the same method as H. A. Bethe, Phys. Rev. 72, 339 (1947), for our renormalization.

PHYSICAL REVIEW A VOLUME 3, NUMBER 3 MARCH 1971

Excitations Radiated from a Thermal Source in Helium II below 0.3K*

R. W. Guernsey,† Jr. and K. Luszczynski‡
Department of Physics, Washington University, Saint Louis, Missouri 63130
(Received 19 October 1970)

Results are presented on the propagation of excitations generated by a small (~1 mm square) pulsed heater immersed in a large (~300 cc) sample of He II maintained at temperatures below 300 mK. Small carbon-film detectors placed at 1, 2, 3, and 4 cm from the heater are used to measure the flux of radiation over a wide range of heater-power densities (W_H). The observed signals are free from wall reflections. At the lowest temperatures and small W_H, the fastest excitations propagate without dispersion or attenuation at a velocity of 234 ± 4 m/sec. Spatial attenuation which is observed at higher temperatures corresponds to effective mean free paths for large-angle scattering of 1, 2, and 3cm at 306 ± 6, 272 ± 6, and 254 ± 8 mK, respectively. When W_H exceeds 0.4 W/cm^2, signal shapes reflecting appreciable interactions between radiated excitations are observed. For $W_H > 2.9$ W/cm^2, the observed signal acquires another component which propagates without appreciable dispersion at a velocity of 200 ± 10 m/sec. In these experiments, no evidence has been found of any excitations associated with any upward bend in the He II phonon-dispersion curve resulting in signal velocities in excess of the first-sound velocity.

I. INTRODUCTION

A heater immersed in He II is expected to generate phonons and other excitations. At sample temperatures above about 600 mK, collisions with intrinsic He II excitations thermalize these emissions to produce the density and temperature fluctuations of first and second sound. At lower temperatures, the intrinsic thermal excitations become rare and direct radiation of phonons from the heater to the detector becomes possible. This paper reports on an experimental study of such signals received at distances of 1–4 cm for input energy fluxes between 0.02 and 8 W/cm^2 and at sample temperatures of 120–900 mK.

There is evidence of direct phonon radiation in past experiments on the transmission of heat pulses down a He II filled tube where one end is the heater and the other a thermometric detector.[1] In such a geometry, however, much of the radiation reaches the detector via reflection from the tube wall. The present experiment is designed to eliminate this complication. A small "point" heater and small detectors are positioned far from the walls in a relatively large sample of He II. At low temperatures corresponding to long mean free path, the signal shape should be indicative of the velocity distribution of the emitted excitations.

This work was originally motivated by a desire to determine the amount of dispersion (if any) in the 50–250-GHz range (energy equal to 2.5–12 K and wave number equal to 0.13–0.66 Å^{-1}) of the phonon spectrum. It is known that the He II liquid structure factor $S(K)$, in the low-temperature limit must have a slope of $1/(2mc)$ as the wave number K approaches 0, where m is the atomic mass of He^4 and c the first-sound velocity.[2] Jackson[3] and Miller *et al.*[2] independently pointed out some time ago

that the measurements of $S(K)$ are compatible with such a limit only if there is a plateau or shoulder somewhere between $K = 0.2$ and 0.8 Å^{-1}. Recent measurements by Hallock[4] do show a gentle shoulder in this range. Jackson calculates that such a shoulder might be reflected as a slight upbend in the phonon-dispersion relation. An 8% increase in the phonon velocity for K between 0.15 and 0.5 Å^{-1} would be consistent with the experimental error reported in the neutron-scattering measurements of the elementary excitation spectrum.[5,6] There have been no studies on the propagation of such high-frequency phonons in He II.

Our experiments show that at sufficiently low heater energy flux (W_H) the radiation seems to consist of a packet of phonons traveling through the liquid without dispersion at 234 ± 4 m/sec. Unfortunately, as the energy flux W_H is raised to levels for which the high-energy phonons should be emitted, significant interactions within the packet set in as reflected by the appearance of anomalous signal shapes. These are discussed here.

II. EXPERIMENTAL DETAILS

A. Source and Detectors

Figure 1 shows the placement of the heater and the detectors. The active area of each element is a square of about 0.9 mm on a side. Detectors A, B, C, and D are located at about 1, 2, 3, and 4 cm, respectively, from the heater H. In each case the line from the center of the heater to the detector

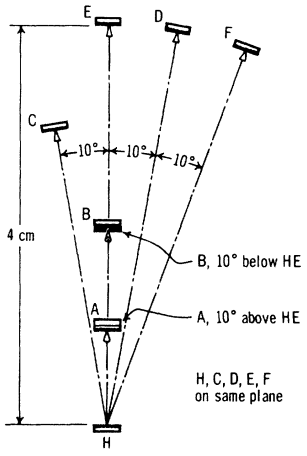

FIG. 1. Schematic illustration of the heater-detector array in the sample cell. Active area of each element is about 0.9×0.9 mm^2. Detectors A, B, C, and D are located at about 1, 2, 3, and 4 cm, respectively, from the heater H. In each case, the line from the center of the heater to the center of the detector is normal to the detector and makes a 10° angle with the heater normal. Additional detectors E and F are placed 4 cm from H; heater-detector center lines HE and HF are inclined at 0° and 20° to the heater normal.

center is normal to the detector and makes a 10° angle with the heater normal. Additional detectors (E and F) are placed at 0 and 20° at the 4-cm distance.

Each element was mounted on a thin post. Fine wire (#44) leads were used, and these were carefully positioned so as not to interfere with the signals. With the exception of the regions behind the heater and the farthest detectors, all objects (mounting plates, container walls, etc.) were at least 2.5 cm from the elements. This ensured that signals reaching the detector via reflection would arrive at least 50% late and be considerably reduced in intensity.

The heater and detectors were prepared from 5-kΩ/square IRC resistance strip which consists of a thin carbon film on a paper-base phenolic laminate. This material has been used often in second-sound experiments. It was cut into 0.9×5-mm strips whose ends were covered with silver paint so as to leave about a 0.9-mm square of carbon in the center. Leads were soldered directly to the paint.

B. Detector Operation and Calibration

In the present experiment, a small dc current (~ 0.4 μA) was maintained through a given detector and the resulting voltage (V) monitored. Power absorbed from an incident phonon flux warmed the film, decreased its resistance, and thus produced a decrease in the monitored voltage. The relationship between this voltage decrement (V') and the absorbed energy flux (W_A) was determined empirically[7] via a steady-state calibration and found to be linear (within 6%) for $W_A \leq 10^{-7}$ W/cm^2. In calibrating some of the larger signals, corrections were made for nonlinearity. An absorbed energy flux of 6×10^{-9} W/cm^2 could be observed with a signal-to-noise ratio of about 1.

It should be emphasized that the above sensitivities have been determined without reference to any particular model for the transfer of energy between the film and the helium. They allow implicitly for heat losses through the film substrate, and they give the *absorbed* energy flux in the steady state. A measurement of the *incident* energy flux requires knowledge of the detector absorption coefficient. This is not known; however, the product of this coefficient and the heater coefficient has been found[7] to be of order 10^{-4}.

C. Cryogenic Procedure

The sample liquid was condensed into the experimental space (cell) from Air Force, Grade-A-well helium gas which should contain about $(1.4 \times 10^{-5})\%$ He^3. After pumping the sample to about 900 mK, the cell was closed off with a special Teflon valve, and the approximately 300 cm^3 of sample were

cooled by adiabatic demagnetization to as low as 120 mK. The data were taken during warm up: The working time to 300 mK was about 1.5 h.

On recycling the system, the heat of magnetization was removed by pumping out some of the sample. When the level fell to within about 2.5 cm of the heater, the run was terminated. The liquid level in the cell was monitored by means of a "second-sonar" technique; that is, by measuring the time for second-sound pulses to travel from a transmitter-receiver at the cell bottom to the surface and back. Temperatures were measured with a Speer carbon resistor of the type investigated by Black, *et al.*[8] This was calibrated against the He^4 vapor pressure (1958 scale) down to 1 K. It is estimated that temperatures so derived are accurate to about ± 3%.

D. Instrumentation

The system used to drive the heater and monitor the detectors was as follows: A manually controlled trigger caused a dc pulse generator to supply a pulse of 1 – 1000-μsec duration to the heater where energy fluxes of 0.025–50 W/cm^2 could be developed. The heater voltage and current pulses were photographed from an oscilloscope so that the power and film temperature could be computed. Decrease in the heater resistance as a result of warming during the input resulted in a maximum power droop of 5%. The input energy fluxes quoted later in this report refer to the midpoint in time. For fluxes ≤ 7 W/cm^2, the power and film temperature changed by less than 2% during input. The rise times were less than 1 μsec. The "fall times" could not be measured, but were probably significantly longer because power must leave the heater via the boundary thermal resistance.

The signals from any two detectors could be displayed simultaneously and photographed on a second oscilloscope whose sweep was triggered at the same time as the pulse generator. Time mark pulses at 1-, 10-, and 100-μsec intervals from the initial trigger were used to modulate the intensity of the scope traces. It was thus possible to measure flight times to a fraction of a microsecond independent of scope sweep calibration and delay.

Photographs of some 1700 signals were made over temperatures of 126–950 mK with input energy fluxes of 0.026–49 W/cm^2 and of duration 10–300 μsec. Most of the data were taken below 300 mK and for inputs of 200 and 300 μsec.

III. DATA AND ANALYSIS

A. Transition from Phonon Radiation to Second Sound

As the sample was warmed from 120 mK to 1 K, the signal velocity was observed to change smoothly from the value expected for individual phonons to that of second sound. Figure 2 shows the flight time measured for the starting point of signals received at the four detector distances (1, 2, 3, and 4 cm) at sample temperatures of 126–950 mK. Decreased signal and reduced detector sensitivity at the higher temperatures made observations impossible at the 3- and 4-cm detectors.

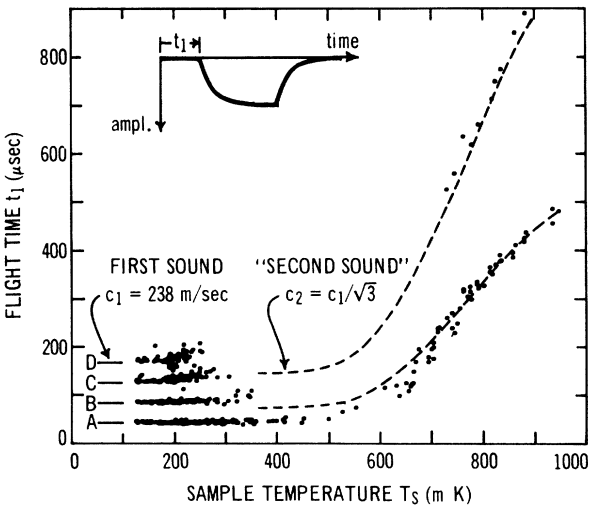

FIG. 2. Flight time t_1 of the signal start at detectors A (1 cm), B (2 cm), C (3 cm), and D (4 cm) plotted against the sample temperature T_S. Solid lines correspond to the flight times expected for first-sound propagation with velocity $c_1 = 238$ m/sec. Dashed lines correspond to second sound [P. J. Bendt *et al.* (Ref. 9)] with an asymptotic value of velocity $c_2 = c_1/\sqrt{3}$, at low temperatures.

The lower-temperature flight times agree well with those expected for low-frequency phonons (solid lines), and above 700 mK the 1- and 2-cm flight times fall reasonably close to the value expected for second sound (dashed lines).[9] One can identify the range from about 500 to 600 mK as the transition region. Here the phonon signal disappears into the noise, and then the second-sound signal emerges. The details of the transition were not apparent because of the smallness of the signal relative to the noise. It should be noted that if the low-temperature signals were thermally generated sound rather than ballistic phonons, then they would have the shape of the first time derivative of the power input.[10]

B. Signals at Low Energy Flux and Low Temperatures

Some 70 signals from the 1-, 2-, 3-, and 4-cm detectors for heater energy-flux values below 0.4 W/cm^2 and sample temperature $T_S < 200$ mK were used in the following analysis. Some examples of the better signals in this region are shown in Fig. 3(a). The shape of the square input pulse is closely reproduced if one takes into account the

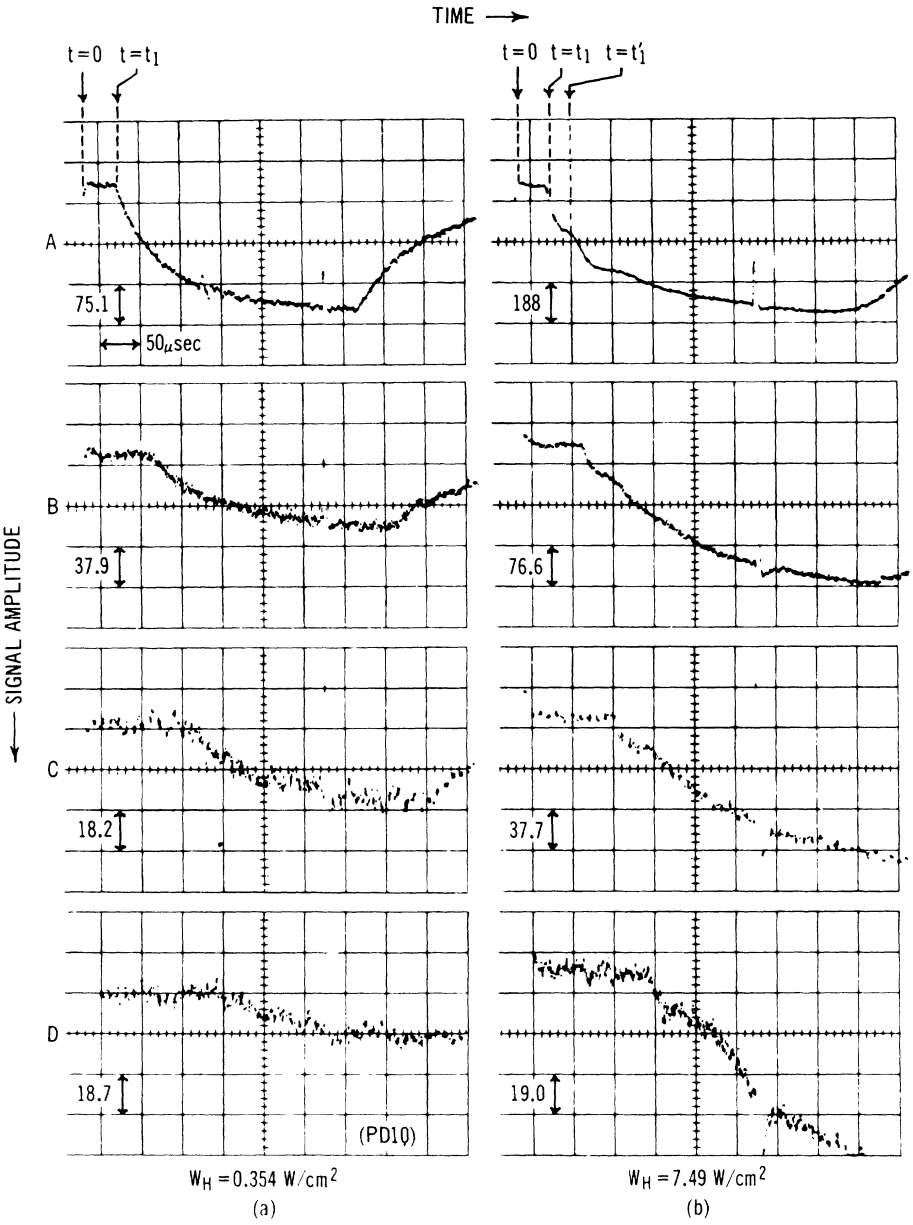

FIG. 3. Photographs of the signals observed at detectors A (1 cm), B (2 cm), C (3 cm), and D (4 cm) for two values of the heater energy flux W_H. (a) $W_H = 0.354$ W/cm^2. The signal propagates without any appreciable dispersion at first-sound velocity (238 m/sec). The signal (onset of the first edge) starts at $t = t_1$. (b) $W_H = 7.49$ W/cm^2. The first edge starts at $t = t_1$ and propagates as in (a) above. The second edge, which appears in the signal at $t = t_1'$, propagates at 200 ± 10 m/sec. The sample temperature range is 126–145 mK. The horizontal sweep is 50 μsec/div. The vertical sensitivity to absorbed energy flux is indicated in each photograph in units of 10^{-9} W/cm^2. The duration of the input pulse is 296 μsec.

limited high-frequency thermal response of the system.

Detailed measurements were made of the maximum amplitude (which is reached at the end of the signal) and of the flight times for the signal start (t_1), the half-amplitude point (t_2), and the turnoff point (t_3). The signal start is taken to be the point at which an extrapolation of the leading edge intersects the center of the baseline noise.

There is no significant dependence of these flight times on the input power or the sample temperature over the restricted ranges under consideration. Figure 4 shows the average flight times measured at the four detectors. These experimental data show that the signal propagates without appreciable dispersion at an average velocity of 234 ± 4 m/sec. This velocity is within experimental error of the accepted sound velocity in He II at low temperature equal to 238 m/sec.[11]

The energy flux being absorbed by the detectors at the end of each signal was determined using the calibration method mentioned in Sec. II B. This was found for each detector to be proportional to the input energy flux. The constants of proportionality were found to vary approximately as the inverse square of the distance. (The best fit exponent was 1.88.)

At higher sample temperatures, the signal am-

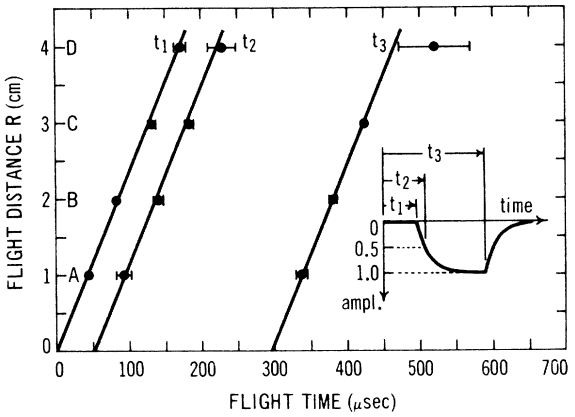

FIG. 4. Distance–vs–flight-time plots for various characteristic points of signals observed at detectors A, B, C, and D, for heater energy flux values $W_H \leq 0.354$ W/cm^2 and sample temperature T_S of 125–197 mK. Plotted points represent average values of flight times of the signal start (t_1), the half-amplitude point (t_2), and the turnoff point (t_3), as indicated in the inset. Length of the error bars is equal to 2σ, where σ is the root-mean-square deviation. Solid lines are drawn with a slope of 234 m/sec.

plitude begins to decline faster than $1/R^2$, where R is the distance from the heater to the detector. This is probably the result of large-angle scattering by background excitations. The signals from the 3- and 4-cm detector became too small to be useful in determining the functional form of this decay, but if it is taken to be $(1/R^2)\, e^{-R/\lambda}$, then the ratio of the signals from the 1-, and 2-cm detectors can be used to determine λ.

The following values of λ are consistent with our observations: 1 cm at 306 ± 6 mK, 2 cm at 272 ± 6 mK, and 3 cm at 254 ± 8 mK. Kramers[1] estimates phonon mean free paths of 4 cm at 340 mK and 10.5 cm at 210 mK from his observations of heat pulses in tubes. One would expect the process limiting his direct signals to be the same as in this experiment, and so his mean free path and the above decay constant should be equivalent. An extrapolation of the present results comes reasonably close to the 210-mK value but is far below the 340-mK result.

C. Signals at High Energy Flux and Low Temperatures

For input energy flux W_H in excess of 0.4 W/cm^2, and sample temperatures below 300 mK, there are marked and significant deviations from the signal characteristics reported above. These are discussed below.

1. *Critical Energy Flux*

For $W_H \leq 3$ W/cm^2 all the signals have similar shapes; however, a plot of the maximum absorbed energy flux W_A versus W_H has a significant decrease in slope between $W_H = 0.36$ and 0.55 W/cm^2. This is shown in Fig. 5, where the results for the A (1-cm) and B (2-cm) detectors are plotted. Similar behavior is seen at the C (3-cm) and D (4-cm) detectors, but the scatter is considerably larger, because of poorer signal-to-noise ratio. The break in the slopes occurs at the same input level but at different signal levels for all the four detectors, implying that the break is characteristic of the source.

Below the break, the slopes of the A and B curves in Fig. 5 are in the ratio of 4:1; this result confirms the $(1/R)^2$ dependence of signal amplitudes for low energy flux and low temperature. Above the break, the slope ratio is 3.0 ± 0.3. The signal amplitude ratio for W_H up to 2 W/cm^2 remains $(1/R)^n$ with $n = 1.9 \pm 0.2$. The signal-start flight times t_1 show no dependence on W_H, but the signal-end flight times t_3 do become slightly longer for higher values of W_H; for example, a 2% increase in this flight time is observed at $W_H = 2$ W/cm^2. It is suspected that this is symptomatic of an increasing effective source size (see Sec. IV).

2. *Second Edge*

With $W_H \geq 2.9$ W/cm^2, a second edge appears early in the signal as shown in Fig. 3(b), and the latter parts of the signal undergo significant shape changes and elongation which will not be considered here. The leading edge of these signals propagates at 234 ± 4 m/sec, and there is little or no delay in its emission, as shown in Fig. 6. The leading edge corresponds most likely to low-energy phonons

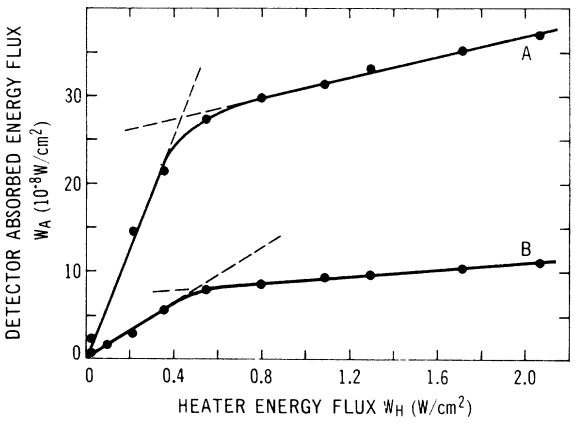

FIG. 5. Relationship between the maximum absorbed energy flux W_A, at detectors A and B, and the heater energy flux W_H represented by the smooth curve drawn through the experimental points. A break in the slope of these curves appears for both detectors when W_H increases above 0.4 W/cm^2. Sample temperature T_S is between 160 and 165 mK.

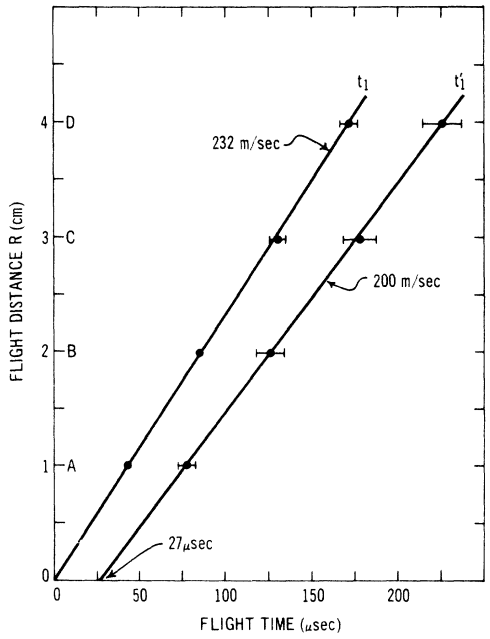

FIG. 6. Distance—vs—flight-time plots for the starting points of the first edge (t_1) and the second edge (t_1') of the signals observed at detectors A, B, C, and D, for heater energy-flux values $W_H \geq 4$ W/cm^2, and sample temperature T_S of 129–218 mK. The first edge is propagated at 232 ± 6 m/sec without any appreciable delay. The second edge is delayed by about 27 μsec and travels with a velocity of 200 ± 10 m/sec. Plotted points represent the average values of flight times measured at each detector. Length of the error bars is equal to 2σ, where σ is the corresponding root-mean-square deviation.

radiated while the heater is warming.

Measurements on 106 signals from the detectors at 1, 2, 3, and 4 cm and for inputs between 4 and 16.2 W/cm^2 show that the start of the second edge (judged as the point at which the curvature of the signal changes sign) has a velocity of about[12] 200 ± 10 m/sec and is emitted about 27 μsec after the start of the heater pulse, as indicated in Fig. 6. The plateau before the second edge has a $(1/R)^2$ amplitude dependence and simply grows longer as the signal propagates outward. When the heater pulse is narrowed to less than 30 μsec, the second edge disappears; this indicates that the delay probably represents the time necessary for the heater to warm to some critical level.

3. *Heater Temperature*

The above phenomena are apparently related to changes in the source behavior. Their full explanation depends on an understanding of the process by which energy is coupled to the helium. As a step in this direction, the heater temperature T_H for pulses of selected power was measured. Figure 7 shows the results. The large error bars allow for the fact that an interpolation of 4.2–77 K was necessary in using the resistance-temperature calibration curve. The heater temperatures are quite high but are not unreasonable in view of the large acoustic mismatch between the carbon and helium. For energy-flux values below about 0.6 W/cm^2 we obtain

$$W_H = [(5.56 \pm 0.65) \times 10^{-6} (\mathrm{W/cm^2})/\mathrm{K^4}] T_H^4$$

above 0.6 W/cm^2, the temperature dependence of W_H is weaker than T_H^4. In other words, for $W_H > 0.6$ W/cm^2, the heater begins to dissipate power less efficiently, and so to radiate the given W_H it must become hotter than the T^4 law would indicate.

IV. DISCUSSION

In the low-energy-flux region with W_H values of 0.025–0.36 W/cm^2, and corresponding heater temperatures of 8–16.5 K, the observed signals are characteristic of direct phonon radiation from a "point" source. Very small-angle scattering causing insignificant change in phonon direction but relaxation of the signal phonon energy distribution could be present. The signal amplitudes are proportional to W_H which is found to be proportional to T_H^4.

For the above range of heater temperatures, the energies of the dominant heater phonons are ex-

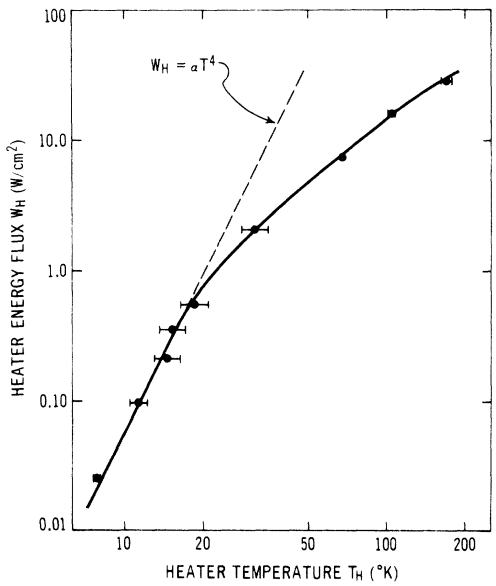

FIG. 7. Relationship between the heater energy flux W_H and the heater temperature T_H represented by the smooth curve drawn through the experimental points. For $W_H \leq 0.6$ W/cm^2, $W_H = [5.56 \times 10^{-6}$ (W/cm^2)/K^4] T_H^4. (The energy flux of 0.6 W/cm^2 corresponds to that of "black body" radiation flux from He II at 0.6 K.)

pected to lie between 22.6 and 46.5 K. However, the He II elementary excitation spectrum does not extend to such high energies. In fact, the phonon branch begins to suffer significant dispersion for energy $E > 10$ K and does not extend above 14 K. If heater phonons only up to 10 K were coupled to helium, then one can show that the radiated energy flux W_H would go approximately as T_H^2 for the range of heater temperatures 8–16.5 K. The observed proportionality of W_H to T_H^4 suggests, therefore, that the entire range of heater phonons is coupled to the helium.

Cowley and Woods[13] have found that inelastic scattering of neutrons from He II for high momentum and energy transfers (up to 1000 K) involves independent-particle-like excitations.[2] If the heater phonons couple to these states with about equal efficiency over most of the distribution, then the rate of heat transfer should be proportional to T_H^4, as is indeed observed. Since the phonon signals are also proportional to T_H^4, it means that a constant fraction (or all) of the energy coupled to the single-particle states ends up as phonon radiation. The single-particle excitations most likely relax quickly to an equilibrium distribution of collective excitations. Thus, the angular and spectral distributions of the radiation from the heater surface should be that of a He II "black body."[7]

While the present experimental results are consistent with the process described above, they do not prove it unequivocally. Additional data on angular and spectral distribution of the radiation are needed. If the signal originates from a local equilibrium distribution of He II phonons at the surface of the heater, then the radiation pattern should show a $\cos(\theta)$ dependence on the angle θ measured from the normal to the heater surface. On the other hand, if the heater phonons are transmitted across the heater surface and propagated in the liquid, then acoustic refraction laws would concentrate the emitted radiation into a small angle about the normal to the surface. (In view of the very short wavelengths involved, this radiation pattern could be observed only if the heater is plane on the atomic scale. The heater used in the present work is not so plane.) Measurement of the spectral distribution of the radiation does not appear to be feasible at this time.

In the present experiment there is no positive indication of any upward bend in the He II phonon-dispersion curve. There are several possible conditions which would contribute to this negative result. If He II "black body" radiation is being observed in the experiment, then for the low-energy-flux values considered above the fraction of phonons in the region of interest would be too small to be detected. Alternatively, if there is direct coupling of phonons from the carbon film to liquid helium, then phonons in the region of interest should have very short lifetimes so that they would decay within a short distance of the source and never reach the detector. It appears, therefore, that the most likely distribution of the resultant radiation would again be that of a He II "black body." Clearly, in this context an estimate of the high-frequency phonon lifetime would give on the order of 10^{-6} sec or less. Small-angle four-phonon scattering with the background phonons might also significantly deplete the number of high-energy phonons on the signal.[14]

In the moderate and high-energy-flux region as W_H is increased above 0.36 W/cm^2, the radiation energy density increases and phonon interactions become more probable. One might expect the first observable effect on the radiation to be a change in its angular distribution. An increasing fraction of the input power should be now scattered out of the forward direction, thus reducing the signal at detectors near the heater normal. If the noninteracting radiation is essentially He II black body radiation, then the signal from the square (side equal a) planar heater of the present experiment should be

$$W_A = a^2 W_H \cos(\theta)/\pi R^2 , \quad R \gg a \tag{1}$$

where R is the detector distance and θ is the angle between the heater-detector center line and the forward direction.

Interactions should first occur adjacent to the heater, and then as W_H is increased this scattering region should grow in all directions from the heater. Some of the phonons interacting beyond the heater edge would be scattered into the backward direction. At high enough input power, the scattering region should become a sphere completely enclosing the heater. Under those conditions there could be no further change in the angular distribution and, by symmetry,

$$W_A = a^2 W_H/4\pi R^2 . \tag{2}$$

The signal now grows at one-fourth the original rate, given by Eq. (1). Here then is a possible explanation of the break in W_A vs W_H. The critical value of W_H, $(W_H)_c = 0.4$ W/cm^2, would be the input energy flux for which the phonon density at the heater is sufficient to give a mean free path for large-angle scattering on the order of the heater dimensions. Such an interpretation is consistent with the attenuation data of Sec. III C. Rough estimates of the scattering expected for input energy fluxes up to 2.9 W/cm^2 suggest signal levels in reasonable agreement with those actually observed. A definitive check of the above model could be made by studying the signal from a uniformly heated spherical source. In this case, there should be no break in the W_A-vs-W_H curves.

The transfer of heat from the carbon film to the

liquid must be clearly affected as W_H is increased above $(W_H)_c$. The increased scattering in the radiation must eventually result in a growing region of local thermal equilibrium at the heater. The local temperature there should rise as increased W_H and additional backscattering of phonons from the outgoing radiation add more excitations to the region. At distances where the phonons are spread over a greater area, and where phonon-phonon scattering is reduced, the equilibrium should be less perfect and finally nonexistent.

A lower limit on the local liquid temperature should be that of an equilibrium distribution capable of radiating energy flux W_H (e.g., $W_H = 2.06$ W/cm^2 would correspond to $T \geq 0.80$ K). The phonons coupling back into the heater from such a distribution will constitute insignificant energy flux compared to W_H, and so there should be no modification of the heater's T^4 radiation law. The deviation from this law, observed for $W_H \geq 0.6$ W/cm^2, must represent impaired coupling of energy from the heater phonons to the liquid. The local temperature at this W_H is greater than 0.6 K, and so rotons are just appearing.[7] Perhaps they affect the coupling process. One could speculate that vortices or even film boiling[15] also is involved. The details appear quite complicated, and so the question will be left open for the present.

Interpretation of the anomalous signal shapes observed at even higher W_H must also wait for a better understanding of the source behavior. Suffice it to say that the 200 ± 10-m/sec second-edge velocity does not agree with that expected for any known mode of energy transfer in He II.[7]

V. CONCLUSIONS

It has been found that a thermal source in a large sample of He II at temperature $T_S < 300$ mK can generate direct phonon radiation with energy-flux values up to 0.4 W/cm^2. This radiation, which is detected by means of heat-sensitive carbon films, is probably characteristic of He II black body radiation corresponding to an equilibrium temperature of 0.54 K; for this temperature, 95% of the phonons have energies below 4.7 K.[7] The observed maximum velocity of thermal excitations is found to be 234 ± 4 m/sec. (The measured sound velocity in He II is 238 m/sec.) Measurements of the spatial signal attenuation as a function of the sample temperature T_S indicate phonon mean free paths for large-angle scattering of 1, 2, and 3 cm at 306 ± 6, 272 ± 6, and 254 ± 8 mK, respectively. No evidence has been found of the faster phonons which should be associated with an upward bend in the dispersion curve. This indicates either that such dispersion does not exist or that, if it does exist, then the faster phonons decayed near the source or were not generated at all.

When the radiation energy flux W_H exceeds 0.4 W/cm^2, phonon-phonon interactions within the signal appear to become significant. These interactions modify the angular distribution of the energy radiated from the heater and lead to an appreciable modification in the growth of the detected signal with increasing W_H. At sufficiently high values of W_H, the interactions result most likely in the formation of a macroscopic region of local thermal equilibrium at the heater. For $W_H \geq 0.6$ W/cm^2, the coupling of energy from the heater to the liquid shows a decreasing efficiency. For $W_H \geq 2.9$ W/cm^2, another edge propagating with velocity of 200 ± 10 m/sec appears in the signal. A detailed explanation of this phenomenon is not yet apparent. Further work on spectral and angular distribution of the radiated excitations in He II is needed to provide a better understanding of the processes involved in the transfer of energy between the heater and He II for a wide range of energy-flux values.

ACKNOWLEDGMENTS

We would like to thank Professor R. E. Norberg for his interest in this work. We are grateful to Dr. J. W. Jackson for numerous valuable discussions.

*Work supported by U. S. Army Research Office (Durham) Grant No. DA-ARO-D-31-124, NASA Grant No. NsG-581, and National Science Foundation Grant No. GU-1147.

†National Science Foundation Graduate Fellow. Present address: Department of Physics, Columbia University, New York, N. Y.

‡Alfred P. Sloan Fellow.

[1]H. C. Kramers, Proc. Acad. Sci. Amsterdam B 59, 35 (1956); 59, 48 (1956).

[2]A. Miller, D. Pines, and P. Noizères, Phys. Rev. 127, 1452 (1962).

[3]H. W. Jackson, Ph. D. thesis, Washington University, St. Louis, 1962 (unpublished); Dissertation Abstr. 24, 1206 (1963).

[4]R. B. Hallock, Phys. Rev. Letters 23, 830 (1969).

[5]D. G. Henshaw and A. D. B. Woods, Phys. Rev. 121, 1266 (1961).

[6]A. D. B. Woods and R. A. Cowley, Phys. Rev. Letters 24, 646 (1970).

[7]R. W. Guernsey, Jr., Ph.D. thesis, Washington University, St. Louis, 1968 (unpublished); Dissertation Abstr. 29, 712-B (1968).

[8]W. C. Black, Jr., W. R. Roach, and J. C. Wheatley, Rev. Sci. Instr. 35, 587 (1964).

[9]P. J. Bendt, R. D. Cowan, and J. L. Yarnell, Phys. Rev. 113, 1386 (1959).

[10]Uno Ingard, in *Handbook of Physics*, edited by E. U. Condon and H. Odishaw (McGraw-Hill, New York, 1958), Vol. III, p. 115.

[11]W. M. Whitney and C. E. Chase, Phys. Rev. 158, 200 (1967).
[12]R. W. Guernsey, Jr. and K. Luszczynski, in *Proceedings of the Eleventh International Conference on Low Temperature Physics, St. Andrews, Scotland*, 1968 edited by J. F. Allen, D. M. Finlayson, and O. M. McCall (University of St. Andrews Printing Dept., St. Andrews, Scotland, 1969), Vol. 1, p. 428
[13]R. A. Cowley and A. D. B. Woods, Phys. Rev. Letters 21, 787 (1968).
[14]I. M. Khalatnikov, *Introduction to the Theory of Superfluidity* (Benjamin, New York, 1965), p. 42.
[15]T. H. K. Frederking, Chem. Eng. Progr. Symp. Ser. 64, No. 87, 21 (1968).

PHYSICAL REVIEW A VOLUME 3, NUMBER 3 MARCH 1971

He^3 Spin Diffusion in Dilute He^3-He II Mixtures at Elevated Pressures in the Semiclassical Regime*

D. K. Biegelsen† and K. Luszczynski‡
Department of Physics, Washington University, Saint Louis, Missouri 63130
(Received 5 October 1970)

Measurements of the spin-diffusion coefficient in dilute He^3–He II mixtures are presented. The thermodynamic parameters of the samples are varied within the following limits: $0.3 \leq T \leq 1.15$ °K, saturated vapor pressure $\leq P \leq 24$ atm, $0.322\times10^{-4} \leq n_3 \leq 4.54\times10^{-4}$ mole/cm^3. It is shown that all samples considered are within the limits of the semiclassical regime. The data are analyzed by considering the reciprocal of the diffusion to be the sum of two parts: $1/D(T,P,n_3) = 1/D_{3\rho}(T,P) + 1/D_{33}(T,P,n_3)$, where $D(T,P,n_3)$ is an experimental measurement at (T,P,n_3), $D_{3\rho}(T,P)$ is the n_3-independent spin diffusion of a He^3 quasiparticle as limited by interactions with rotons, and $D_{33}(T,P,n_3)$ is the spin diffusion of a He^3 quasiparticle limited by interactions with other He^3 quasiparticles. Since $D_{3\rho}$ is independent of n_3, and D_{33} is shown to be proportional to n_3^{-1}, a least-squares fit of the data to the above equation gives the experimentally determined values of $D_{3\rho}$ and D_{33}. A comparison of D_{33} with the theoretical expression gives directly the moment of the effective He^3–He^3 interaction measured by spin diffusion in the semiclassical regime: $\langle V(k)\rangle|_{T,P} = A\int e^{-ak^2}k^3|V(bk)|^2\,dk$, where A, a, and b are constants. The measurements are insufficient to determine $V(k)$ uniquely. Calculations using an assumed interaction (which reduces to the interaction used by Ebner at saturated vapor pressure) show a remarkable similarity to the experimental data.

I. INTRODUCTION

The properties of dilute He^3–He II mixtures can be explained quite well theoretically in two thermodynamic regions, the Fermi degenerate regime and the semiclassical regime. In this paper experimental measurements of the spin-diffusion coefficient covering most of the semiclassical regime are presented and related to the effective quasiparticle interactions.

The properties of dilute mixtures were treated first phenomenologically by Landau and Pomeranchuk.[1] They suggested that well below the λ-transition temperature ($T \lesssim 1.5$ °K) the solutions can be considered as a mixture of three dilute quasiparticle gases in a superfluid background: The He^4 (Bose) excitations are taken to be phonons and rotons with dispersion relations $\epsilon(k) = \hbar ck$ and $\epsilon(k) = \Delta + \hbar^2(k-k_0)^2/2\mu_\rho$, respectively, where $\hbar$ is Planck's constant divided by 2π, c is the velocity of sound in He^4, Δ is the roton excitation energy, k_0 is the magnitude of the roton momentum at the energy minimum, and μ_ρ is the roton effective mass; the He^3 (Fermi) quasiparticles are taken to have dispersion $\epsilon(k) = E_3 + \hbar^2k^2/2m_3^*$, where m_3^*, the quasiparticle effective mass, is determined empirically. The degeneracy temperature of the quasiparticle gas is

$$T_F = \hbar^2k_F^2/2m_3^*k_B = \hbar^2(3\pi^2n_3)^{2/3}/2m_3^*k_B\ ,$$

where n_3 is the He^3 number density, k_F is the Fermi momentum, and k_B is Boltzmann's constant. The semiclassical regime comprises a region of the thermodynamic phase space in which the quasiparticle gases are (i) dilute, (ii) nondegenerate (approximately Boltzmann), and (iii) only weakly interacting. The region can be defined by $2T_F \lesssim T \lesssim 1.5$ °K, $0 < x \lesssim 5\%$, and $\mathrm{SVP} \leq P \leq P_{\mathrm{melting}}$, where x is the molar concentration, P is the pressure, and SVP is the saturated vapor pressure. (The last two limits can be specified also in terms of the independent thermodynamic variables n_3 and n_4. Above 1.5 °K and/or 5%, the quasiparticle gases can no longer be considered dilute.) Khalatnikov and Zharkov[2] have obtained theoretical expressions for the transport properties of the mixtures assuming δ-function interactions for He^3-He^3, He^3-roton, and roton-roton scattering. For He^3-He^3 scattering processes, at least, experiments show that more realistic interactions must